2-2013

Pair creation for bosons in electric and magnetic fields

Q Z. Lv
China University of Mining and Technology

A C. Su
Illinois State University

M Jiang
Chinese Academy of Sciences

Rainer Grobe
Illinois State University

Qichang Su
Illinois State University

Pair creation for bosons in electric and magnetic fields

Q. Z. Lv,[1] A. C. Su,[2] M. Jiang,[3] Y. J. Li,[1] R. Grobe,[2] and Q. Su[2]

[1]*State Key Laboratory for Geomechanics and Deep Underground Engineering, China University of Mining and Technology, Beijing 100083, China*
[2]*Intense Laser Physics Theory Unit and Department of Physics, Illinois State University, Normal, Illinois 61790-4560, USA*
[3]*Beijing National Laboratory for Condensed Matter Physics, Institute of Physics, Chinese Academy of Sciences, Beijing 100190, China*

By solving the quantum field theoretical version of the Klein-Gordon equation numerically, we study the creation process for charged boson-antiboson pairs in static electric and magnetic fields. The fields are perpendicular to each other and spatially localized along the same direction, which permits us to study the crucial impact of the magnetic field's spatial extension on dynamics. If its width is comparable to that of the electric field, we find a magnetically induced Lorentz suppression of the pair-creation process. When the width is increased such that the created bosons can revisit the interaction region, we find a region of exponential self-amplification that can be attributed to a spontaneous emissionlike enhancement. If the width is increased further, this trend is reversed and the magnetic field can even shut off the particle production completely.

I. INTRODUCTION

In view of the recent development of high-powered laser systems, the creation process of electron-positron pairs from the vacuum in a supercritical external field has gained considerable attention in the research community. Various laser and other external field configurations have been studied with the goal to lower the threshold for this process. Historically, the creation of electron-positron pairs was first investigated by Sauter [1] and Schwinger [2]. These works considered the effect of a static electric field and triggered the attention to this fascinating research area.

Since then many studies [3] have followed and extended the pair-creation conditions from a constant electric field to electromagnetic fields with more general space- and time-dependent pulse shapes. In most of the early research, the magnetic field was neglected as its effects on fermions are usually smaller compared to that of the electric field [4]. However, as the experimentally achievable laser intensities have steadily increased [5], this field can no longer be neglected.

The electron-positron pair-creation process characterizing the supercritical breakdown of the fermionic vacuum is a striking prediction of the Dirac equation [6]. It turns out that a quantum field theory based on the Klein-Gordon equation predicts a similar breakdown process leading, in this case, to the creation of boson-antiboson pairs. This process has not been studied as widely, as the required field strength to trigger such a process is considered to be even larger than the one for breaking down the fermionic vacuum. The threshold strength is related to the rest energy of the created particles and a π meson is about 270 times as heavy as an electron. We will argue below that the study of the analogous bosonic processes can also give us additional knowledge on dynamics that cannot be gathered from the fermionic pair creation.

Most of the theoretical techniques to study the pair-creation process rely on perturbative expansions and the determination of the S matrix to study the long-time behavior. These methods can be modified to study different field configurations. Alternatively, a space-time resolved computational approach permits us to examine position-dependent mechanisms, in-

cluding the short-time dynamics. With this approach we have phrased general fundamental questions concerning the pair-creation process. With the inclusion of the magnetic field this framework becomes more involved as the underlying particle motion is intrinsically multidimensional.

In a recent work [7] we have shown that the presence of a minute magnetic field that is perpendicular to the electric field can completely suppress the pair-creation rate for fermions. We have suggested that this suppression could have multiple causes. One of these is the Lorentz reduction [8–10], which is based on the observation that in the special case of spatially homogeneous fields one can find a Lorentz transformed new coordinate frame, in which the magnetic field is zero and the electric field is always smaller than the original electric field. A second physical mechanism for the suppression is possible, as the magnetic field can return the created fermions to the interaction zone, which then could decrease the production as a consequence of the Pauli blocking principle [11–16]. It is difficult to discriminate between these two mechanisms within a purely fermionic framework as they both lead to the same suppressive effect. If the Pauli blocking is really relevant, would we not expect an amplification of the pair creation if we simply replaced the fermions with bosons, as they obey the opposite particle statistics? In fact, in prior works [17,18] we have argued that the direct counterpart of the usual Pauli blocking for fermions is the spontaneous emissionlike amplification for the analogous bosonic system. This open question is one of the motivations for us to study the supercritical creation process for bosons in a magnetic field.

In this work, we attempt to build a general computational framework to calculate the bosonic particle-antiparticle pair-creation process in electromagnetic fields that are both time dependent and spatially inhomogeneous. In particular, we examine inhomogeneous fields where the electric and magnetic components are perpendicular to each other and their magnitude varies only in one dimension. We will show below that there are three distinct regimes of interactions depending on the spatial extension of the magnetic field. As we increase this extension, we first change from the predicted Lorentz

suppression to a regime of exponential self-amplification and finally enter a region where the magnetic field can shut off the particle production altogether. This nonmonotonic behavior is rather unexpected and interesting as the trends are completely reversed twice. It is therefore even qualitatively different from the monotonic behavior of fermions.

This work is organized as follows. In Sec. II, we describe the quantum field theoretical method used to solve the Klein-Gordon equation and calculate the bosonic particle-antiparticle creation process in electromagnetic fields. In Sec. III, we compare the pair-creation yields of fermions and bosons without any magnetic field and compare them with the predictions of Schwinger's formula [2]. In Sec. IV we examine the special case where both fields have identical spatial distributions. We also compare the exact data with the expressions based on a generalized Hund formula [19]. In Sec. V we study the exponential self-amplification regime. In Sec. VI we show how the magnetically induced shut-off mechanism [7], [20] can be traced back to qualitative changes in the underlying energy spectra. Finally, in Sec. VII we summarize and give an outlook on some interesting open questions.

II. QUANTUM FIELD THEORY OF PAIR CREATION FOR BOSONIC SYSTEMS

The study of the pair creation in external fields requires the framework of quantum field theory. Former works have focused on the fermionic pair-creation processes in an electric field only, but recently we have extended this framework to allow the external field to have both electric and magnetic field components [7,20]. The Dirac equation was second quantized within a Hilbert space of magnetic field dressed states. In this work, we also second quantize the Klein-Gordon equation in a Hilbert space of basis states dressed by the magnetic field.

A. The first-order Klein-Gordon equation

The Klein-Gordon equation for bosons is usually given as a second-order differential equation in time for $\psi(r,t)$,

$$\frac{1}{c^2}\frac{\partial^2 \psi}{\partial t^2} = \left(\frac{\partial^2}{\partial x^2} + \frac{\partial^2}{\partial y^2} + \frac{\partial^2}{\partial z^2} - c^2\right)\psi. \quad (2.1)$$

We choose atomic units from now on. The usual form of the Klein-Gordon equation can be transformed into a set of two coupled differential equations [21,22] that are first order in time. The transformation can be achieved by the ansatz

$$\psi = \phi + \chi, \quad (2.2)$$

$$i\frac{\partial \psi}{\partial t} = c^2 (\phi - \chi). \quad (2.3)$$

One can easily show that Eq. (2.1) is equivalent to the set of two coupled differential equations that are first order in time:

$$i\frac{\partial \phi}{\partial t} = -\frac{1}{2}\nabla^2 (\phi + \chi) + c^2\phi,$$
$$i\frac{\partial \chi}{\partial t} = \frac{1}{2}\nabla^2 (\phi + \chi) - c^2\chi. \quad (2.4)$$

The resulting two equations turn out to be more convenient for numerical calculations and also allow for a more direct comparison with the Dirac equation for fermions. The coupled

equations (2.4) can be combined to a single equation for the two-component column vector $\Psi = \begin{pmatrix} \phi \\ \chi \end{pmatrix}$. If we introduce the Pauli matrices σ_i, we can rewrite the Klein-Gordon equation as a Schrödinger-like equation with a Hamiltonian:

$$H_{KG} = (\sigma_3 + i\sigma_2)\frac{\hat{p}^2}{2} + \sigma_3 c^2 = N\frac{\hat{p}^2}{2} + \sigma_3 c^2. \quad (2.5)$$

Here the nilpotent matrix is defined as $N = \begin{pmatrix} 1 & 1 \\ -1 & -1 \end{pmatrix}$ and the two-component KG equation can be written in a compact form as

$$i\frac{\partial}{\partial t}\Psi = H_{KG}\Psi. \quad (2.6)$$

The Hamiltonian is only generalized Hermitian [21,22] but the corresponding time evolution preserves the normalization of the form

$$\int \Psi^\dagger \sigma_3 \Psi \, d^3x = \int (\phi\phi^* - \chi\chi^*) d^3x. \quad (2.7)$$

Using the Kein-Gordon Hamiltonian equation (2.5), we can compute the positive and negative energy solutions of free particles separately:

$$E = +E_p,$$
$$\langle \mathbf{x}|p\rangle = \Psi^+(\mathbf{x}) = \frac{1}{\sqrt{4E_p c^2}}\begin{pmatrix} c^2 + E_p \\ c^2 - E_p \end{pmatrix}\frac{e^{i\mathbf{p}\cdot\mathbf{x}}}{\sqrt{(2\pi)^3}}, \quad (2.8)$$

$$E = -E_p,$$
$$\langle \mathbf{x}|n\rangle = \Psi^-(\mathbf{x}) = \frac{1}{\sqrt{4E_p c^2}}\begin{pmatrix} c^2 - E_p \\ c^2 + E_p \end{pmatrix}\frac{e^{i\mathbf{p}\cdot\mathbf{x}}}{\sqrt{(2\pi)^3}}, \quad (2.9)$$

where $E_p = c\sqrt{(c^2 + p^2)}$. These energy-momentum eigenstates can be used to expand the corresponding field theoretical operators that contain creation and annihilation operations.

B. The coupling of the bosons to an electromagnetic field

Using the minimal coupling principle, the Klein-Gordon equation (2.6) can be generalized to include the interaction with an external electromagnetic field

$$i\frac{\partial}{\partial t}\Psi = \left[\frac{N}{2}\left(\hat{p} + \frac{\mathbf{A}}{c}\right)^2 + \sigma_3 c^2 + V\right]\Psi. \quad (2.10)$$

A changing magnetic field always leads to an electric field, which could affect the pair-creation process and modify the number of particle pairs. In order to avoid this unnecessary complication associated with the turn on and turn off of the vector potential $\mathbf{A}$, we assume that the magnetic field is time independent. In practical terms this means that the magnetic field is turned on slowly before the supercritical electric field pulse. In order to describe the created pairs, we first consider the (time-independent) vector potential in the Klein-Gordon Hamiltonian without any electric field ($V = 0$):

$$h^A = \frac{N}{2}\left(\hat{p} + \frac{\mathbf{A}}{c}\right)^2 + \sigma_3 c^2. \quad (2.11)$$

We can use its eigenvectors to construct an orthonormal basis set satisfying

$$h^A \psi_P^A(\mathbf{x}) = E_P^A \psi_P^A(\mathbf{x}),$$
$$h^A \psi_N^A(\mathbf{x}) = E_N^A \psi_N^A(\mathbf{x}). \quad (2.12)$$

The subscripts P and N denote positive and negative energy eigenstates $\psi_P^A(\mathbf{x})$ and $\psi_N^A(\mathbf{x})$, respectively. Note that there is a gap between the positive and negative continuum, which is related to the fact that a static magnetic field by itself cannot create particles. This will be discussed in more detail below in Sec. VI. Using this basis set, the field operator can be expanded as

$$\hat{\Psi}(\mathbf{x},t) = \sum_P \hat{B}_P(t)\psi_P^A(\mathbf{x}) + \sum_N \hat{D}_N^\dagger(t)\psi_N^A(\mathbf{x}), \qquad (2.13)$$

where $\hat{B}_P(t)$ and $\hat{D}_N^\dagger(t)$ are the annihilation and creation operators for positive and negative states at time t, respectively. Please note that we have replaced the usual integration over the momentum space by a discrete sum to reflect our numerical momentum grid. As a result, the bosonic commutation relations are given in terms of the Kronecker symbol and not the Dirac delta function, $[\hat{B}_{P_1}(t), \hat{B}_{P_2}^\dagger(t)] = \delta_{P_1,P_2}$ and $[\hat{D}_{N_1}(t), \hat{D}_{N_2}^\dagger(t)] = \delta_{N_1,N_2}$ making these operators unitless.

In order to construct the time evolution of the field operator, we have solved the time-dependent Klein-Gordon equation $i(\partial/\partial t)\phi(\mathbf{x},t) = h(t)\phi(\mathbf{x},t)$ under the full Hamiltonian

$$h(t) = \frac{N}{2}\left(\hat{p} + \frac{\mathbf{A}}{c}\right)^2 + \sigma_3 c^2 + V, \qquad (2.14)$$

where we have used the eigenstates from Eq. (2.12) as initial states $\phi(\mathbf{x},t=0) = \psi_{P,N}^A(\mathbf{x})$. We can therefore expand the field operator [equivalently to Eq. (2.13)] in terms of these solutions as

$$\hat{\Psi}(\mathbf{x},t) = \sum_P \hat{B}_P\phi_P(\mathbf{x},t) + \sum_N \hat{D}_N^\dagger\phi_N(\mathbf{x},t). \qquad (2.15)$$

Comparing Eqs. (2.13) and (2.15), one can obtain the relationship between the time-dependent operators $\hat{B}_P(t)$, $\hat{D}_N^\dagger(t)$ and their time-independent counterparts $\hat{B}_P, \hat{D}_N^\dagger$:

$$\hat{B}_P(t) = \sum_Q U_{P,Q}(t)\hat{B}_Q + \sum_M U_{P,M}(t)\hat{D}_M^\dagger,$$
$$\hat{D}_N^\dagger(t) = \sum_Q U_{N,Q}(t)\hat{B}_Q + \sum_M U_{N,M}(t)\hat{D}_M^\dagger, \qquad (2.16)$$

where we denote the matrix coefficient as $U_{\xi,\zeta}(t) = \langle\psi_\xi^A(\mathbf{x}) \mid \phi_\zeta(\mathbf{x},t)\rangle$, where ξ and ζ denote P or N. The main task in computing the matrix element is to calculate the time-dependent evolution of the Hamiltonian with full interaction. Such a numerical procedure can be accomplished with the split operator technique.

From the above relation we can compute the quantum field theoretical quantities at any time t. For example, if we consider the vacuum state $|0\rangle$ in the magnetic field as our initial state, we can compute the total number of the created bosons and

their spatial density as

$$N(t) = \langle 0|\int d^3x\, \hat{\Psi}_+^\dagger(\mathbf{x},t)\hat{\Psi}_+(\mathbf{x},t)|0\rangle$$
$$= \langle 0|\sum_P \hat{B}_P^\dagger(t)\hat{B}_P(t)|0\rangle$$
$$= \sum_P \sum_N |U_{P,N}(t)|^2 \qquad (2.17)$$

and

$$\rho(\mathbf{x},t) = \langle 0|\hat{\Psi}_+^\dagger(\mathbf{x},t)\hat{\Psi}_+(\mathbf{x},t)|0\rangle$$
$$= \langle 0|\sum_{PP'} \hat{B}_P^\dagger(t)\psi_P^{A\dagger}(\mathbf{x})\hat{B}_{P'}(t)\psi_{P'}^A(\mathbf{x})|0\rangle$$
$$= \sum_N \left|\sum_P U_{P,N}(t)\psi_P^A(\mathbf{x})\right|^2. \qquad (2.18)$$

Here the subscript "$+$" denotes the boson (and not antibosonic) portion of the corresponding operator.

If we choose the special vector potential $\mathbf{A} = (0, A_y(x), 0)$ and scalar potential $V = V(x,t)$ the Hamiltonian $h(t)$ can be written in a simpler form as

$$h(t) = \frac{N}{2}\hat{p}_x^2 + \frac{N}{2}\left(\hat{p}_y + \frac{A_y(x)}{c}\right)^2 + \sigma_3 c^2 + V(x,t), \qquad (2.19)$$

where we neglect the trivial z-dependence.

It is easy to check that the operator $\hat{p}_y$ commutes with $h(t)$ thus making the canonical momentum p_y a conserved quantity. We can expand the wave function of Hamiltonian h^A into different components of p_y before summing up the contribution due to different p_y, as $\psi_\xi^A(\mathbf{x}) = \sum_{p_y} \varphi_\xi^{A,p_y}(x)e^{ip_y y}/\sqrt{L_y}$. Here L_y denotes the numerical box length in the y direction and the subscript ξ denotes again P or N. Finally, applying the general prescription of Eqs. (2.17) and (2.18) to our two-dimensional case we can compute the total number of created particles per unit length along the y direction $N(t)$ and the spatial density $\rho(x,y,t)$ as

$$N(t) = \sum_{P,N,p_y} \left|U_{P,N}^{p_y}(t)\right|^2 / L_y = \int dx\, \rho(x,y,t), \quad (2.20)$$

$$\rho(x,y,t) = \sum_{p_y,N} \left|\sum_P U_{P,N}(t)\varphi_P^{A,p_y}(x)\frac{e^{ip_y y}}{\sqrt{L_y}}\right|^2. \quad (2.21)$$

Note that $\rho(x,y,t)$ depends only on x. As the external fields are infinitely extended along the y direction the total number of particles would be infinite and we therefore consider all quantities relative to L_y. The conservation of p_y permits us to reduce the spatial dimension of the calculation, which significantly decreases the required computational time to only a few days. In fact, without this conservation, an *ab initio* field theoretical simulation for spatially inhomogeneous electric and magnetic fields would be rather difficult—if not impossible.

To have specific electric and magnetic fields for our simulations, we assume that they are represented by the scalar potential $V(x) = V_0[1 + \tanh(x/W_E)]/2$ and vector potential

$\mathbf{A}(x) = A_0(0,[1 + \tanh(x/W_B)]/2, 0)$, respectively [1]. These forms correspond to an E and B field pointing in the x and z directions, respectively. Both fields are spatially localized along the x direction around $x = 0$ with widths of W_E and W_B. The corresponding fields are obtained as $E(x) = -dV(x)/dx$ and $B(x) = dA_y(x)/dx$. The fields are largest at $x = 0$, where $E(x) \sim V_0/(2W_E)$ and $B(x) \sim A_0/(2W_B)$. The corresponding peak scalar and magnetic potentials V_0 and A_0 can be expressed in units of c^2, the electric and magnetic field widths W_E and W_B in units of $1/c$, and the electric and magnetic fields E and B are given in units of c^3.

While spatially inhomogeneous fields usually make most standard theoretical approaches more difficult, they provide the advantage of allowing us to examine the dynamics from a spatially resolved perspective. The system is initially in the vacuum state $|0\rangle$ associated with the inhomogeneous magnetic field. The electric field is then turned on to initiate the pair-creation process. The calculations are performed on a space-time lattice with up to 1024 grid points in the x direction and 10 000 temporal points. Each simulation is then repeated for 1024 values of the momentum p_y, making the calculation effectively two dimensional [20].

III. PAIR CREATION FOR BOSONIC AND FERMIONIC SYSTEMS FOR $B = 0$

The main difference between bosons and fermions is the commutation relation that the field operators have to fulfill. In this section, we will compare the corresponding time-dependent particle numbers for fermions and bosons without the magnetic field. We will also discuss alternative theoretical frameworks based on the works of Schwinger and Hund that can predict the pair-creation rate in the long-time limit. The dynamics of the electron-positron pairs are described by the Dirac equation. Details about its solution and properties can be found abundantly in the literature [23–26]. For a better comparison we assume here that the bosons and fermions have the same mass, which was chosen to be 1 in atomic units.

In Fig. 1 we have graphed the temporal growth of the number of fermion and boson pairs for three different spatial extensions W_E of the supercritical electric field strength $E_0 = 1.5c^3$. For short times $N(t)$ reflects the sudden turn on of
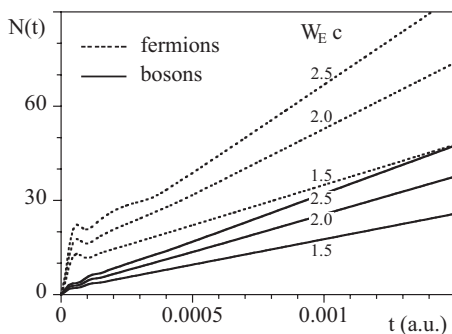

FIG. 1. The total number of created bosons and fermions as a function of time t for bosonic and fermionic systems and three extensions of the electric field W_E [electric field amplitude $E_0 = V_0/(2W_E) = 1.5c^3$; numerical box size $L = 1$ with 512 spatial grid points].
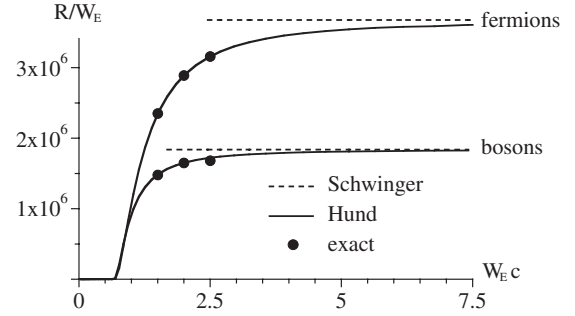

FIG. 2. The "normalized" long-time pair-creation rate R/W_E as a function of the field width W_E. The dashed lines are calculated from Eqs. (3.1) and (3.2). The solid curves are calculated from Eq. (3.3) and include all possible canonical momenta p_y [same parameters as in Fig. 1].

the electric field. For reasons that are presently unclear, more fermions (dashed lines) than bosons are created in this early time domain. However, for longer times $N(t)$ grows linearly in each of the six cases and the slopes of $N(t)$ for the fermions exceed those for the bosons for this particular parameter range. As we have fixed the strength of the electric field, an increase of the width W_E requires an increase of the potential V_0. As a result, $N(t)$ as well as the slope of $N(t)$ increases with the spatial size of the interaction region as expected.

In order to compensate the dependence of the slope R on the spatial size of the field, we have computed an effective pair-creation rate per unit length by dividing the numerically determined slopes of the six graphs in Fig. 1 by the width W_E of the interaction region. In Fig. 2 we have graphed these six effective rates R/W_E as a function of the field width. If the width W_E is less than $0.7/c$, the long-time rate vanishes as the field is not supercritical and cannot create any permanent flux of particles. We see that even the "normalized" rate R/W_E depends nontrivially on W_E, reflecting an interesting finite-size effect. Only for large W_E does this rate become independent of W_E.

In Fig. 2 we also compare the exact rates with the predictions of two approximate alternative theories, given by Hund and Schwinger. The famous Schwinger formula is exact only for the special case of an infinitely extended constant electric field. Furthermore, it cannot predict a total yield, which would be infinite at any time for even an infinitesimal field strength. However, it can predict a rate per unit length, which we denote by Γ below.

In order to apply the Schwinger formula to a realistic situation where the electric field is inhomogeneous and has a nontrivial dependence on the position, we have replaced the electric field amplitude in the first term of the original expression by its position-dependent form $E = E(x)$. In two spatial dimensions the number of created particles per unit area and time is

$$\Gamma_B(x) = \frac{E(x)^{3/2}}{4\pi^2 c^{1/2}} \exp\left[-\frac{\pi c^3}{E(x)}\right], \qquad (3.1)$$

$$\Gamma_F(x) = \frac{E(x)^{3/2}}{2\pi^2 c^{1/2}} \exp\left[-\frac{\pi c^3}{E(x)}\right]. \qquad (3.2)$$

The difference between the two systems is simply a factor of 2, reflecting the spin of 1/2 for fermions and 0 for the bosons. In

order to obtain a rate per unit length along the y direction to be compared to our situation, we have integrated both functions over x, leading to $R_{F,B} = \int dx \Gamma_{F,B}(x)$. In order to compare it with the numerical data R/W_E, we have also divided $R_{F,B}$ by W_E. The two horizontal dashed lines in the figure are the predictions associated with the Schwinger formula. They are independent of the width as the Schwinger expression depends only on one single parameter (the electric field E), while the true rate for a localized field depends on the entire spatial profile of the field.

The two continuous graphs in the figure are the predictions of Hund's formula, which is obviously more accurate than Schwinger's expression if the width of the field is not infinitely large. According to Hund the long-time limit of the pair-creation rate can be obtained in one spatial dimension from a quantum mechanical analysis of how an incoming particle with energy E would scatter off the same supercritical field configuration. The rate originally postulated by Hund [19] for $B = 0$ is obtained from the energy integral over the transmission coefficient:

$$R = \frac{1}{2\pi} \int_{E_{\min}}^{E_{\max}} T(E)\,dE. \qquad (3.3)$$

While this simple expression was conjectured by Hund for the case of an electric field only, it turns out that one can generalize it here to include a magnetic field. This will be important for the discussion in Sec. IV. For a nonvanishing magnetic field, we have to include the contributions due to different momentum values and can define a momentum specific rate

$$R(p_y) = \frac{1}{2\pi} \int_{E_{\min}}^{E_{\max}} T_{p_y}(E)\,dE, \qquad (3.4)$$

where $E_{\min} = \sqrt{[c^4 + c^2 p_y^2]}$ and $E_{\max} = V_0 - \sqrt{[c^4 + c^2(p_y + A_0/c)^2]}$. This integration interval ensures that the energies of the states are in the so-called Klein region. In order to apply this expression to fermions with up and down spins, we have to multiply the resulting rate by a factor of 2 and add up contributions due to all p_y, giving $R_F = 2\sum_{p_y} R(p_y)$. One could use various techniques to obtain the transmission coefficient T for a given incoming particle energy. For this work we have adopted the so-called quantum transmitting boundary method. For details about this method [27] we refer the reader to the Appendix.

In order to make the comparison of the exact rate [obtained by dividing the slope of $N(t)$ in the long-time limit by W_E] and the Hund rule more quantitative than depicted in Fig. 2, we have summarized the numerical values in Table I.

We note that in this domain, the Hund formula predicts a creation rate that coincides with the numerical rate of pair production with amazing accuracy. The difference between the Hund formula and the numerical simulations is less than 3%.

IV. LORENTZ SUPPRESSION IN COMBINED *E* AND *B* FIELDS OF SMALL AND EQUAL WIDTHS $W_B = W_E$

In this section, we include the magnetic field and calculate the bosonic particle-antiparticle pair-creation process for the special case where the magnetic and electric fields have equal

TABLE I. The pair-creation rate per unit length from the two methods (parameters as in Fig. 2).

Field width W_E	System	Numerical slope$/W_E$	Hund formula rate$/W_E$
$1.5/c$	Fermion	2.347×10^6	2.343×10^6
	Boson	1.483×10^6	1.484×10^6
$2.0/c$	Fermion	2.890×10^6	2.890×10^6
	Boson	1.648×10^6	1.652×10^6
$2.5/c$	Fermion	3.086×10^6	3.161×10^6
	Boson	1.680×10^6	1.723×10^6

width, $W_E = W_B \equiv W$. We will also assume that this width is smaller than the excursion distance of the particles in the magnetic field for the relevant energies.

In Fig. 3 we show the temporal growth of the total number of bosons for four different sets of parameters. The graph labeled (a) in the figure acts as a reference curve as it corresponds to a magnetic field strength of zero. In graph (b) the magnetic field has an amplitude of $B = 0.6c^3$. We find that the presence of the B field *reduces* the boson-antiboson pair-creation yield for our case where $W_E = W_B$. We will show below that this suppression can be understood in terms of the lowering of an effective electric field when viewed from a different Lorentz frame.

The graph labeled (d) is for the same electric and magnetic field strength, but the spatial extension of the interaction zone has been increased from $W_E = W_B = 0.3c^{-1}$ to $0.5c^{-1}$, while keeping the electric field the same. As a result the pair-creation yield has increased significantly. In order to increase W the corresponding amplitudes of the vector and scalar potentials had to be increased as well. In contrast, in (c) we kept V_0 constant and as a result the pair creation is reduced from (b).

The linear growth of all four graphs in the long-time limit suggests that the slopes can be described by a single rate even for nonvanishing magnetic fields. Following a more quantitative analysis as in the prior section, we have summarized these rates in Table II.

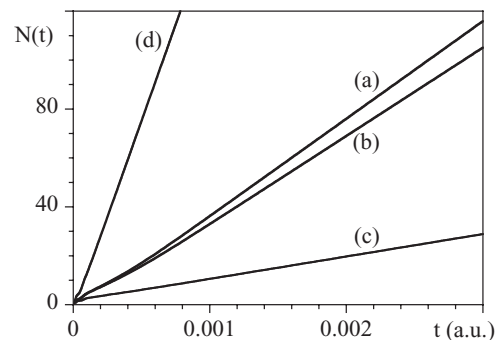FIG. 3. The number of created bosons as a function of time for various field configurations ($L = 1$). Parameters are as follows:

	V_0/c^2	E/c^3	$W_E c$	A_0/c^2	B/c^3	$W_B c$
(a)	2.5	4.17	0.3		0	
(b)	2.5	4.17	0.3	0.36	0.6	0.3
(c)	2.5	2.5	0.5	0.6	0.6	0.5
(d)	4.17	4.17	0.5	0.6	0.6	0.5

TABLE II. The effective pair-creation rates for the data shown in Fig. 2.

Data	Numerical slope	Hund formula
(a)	39777.19	39940.79
(b)	35975.68	36127.74
(c)	9066.06	9170.80
(d)	157667.53	157614.51

As suggested in Sec. III, it turns out that the framework originally proposed by Hund in terms of the energy integral over the quantum mechanical transmission coefficient can be generalized to include the magnetic field. If A_y has the same spatial dependence on x as V, we can Lorentz transform the vector and scalar potential system along the y axis to a new frame, in which the new vector potential A' vanishes. The resulting new scalar potential V' can be used to compute the transmission coefficient of the corresponding quantum mechanical scattering system.

$$\begin{pmatrix} V' \\ A'_x \\ A'_y \\ A'_z \end{pmatrix} = \begin{pmatrix} \gamma & 0 & -\beta\gamma & 0 \\ 0 & 1 & 0 & 0 \\ -\beta\gamma & 0 & \gamma & 0 \\ 0 & 0 & 0 & 1 \end{pmatrix} \begin{pmatrix} V \\ A_x \\ A_y \\ A_z \end{pmatrix}. \quad (4.1)$$

For the data for our graph (b) we require the Lorentz factor $\beta = v/c = -A_y/V = -A_0/V_0 = -0.144$ and $\gamma = 1\sqrt{[1 - \beta^2]} = 1.02$. After this transformation, the new fields are $A'_y = \gamma(\beta V + A_y) = 0$ and $V' = \gamma(V + \beta A_y) = \sqrt{[V_0^2 - A_0^2]} [1 + \tanh(x/W)]/2$. Thus there is no magnetic field in the new inertial frame but an electric field with the same spatial dependence, except that the new potential is lower, $V_{\text{eff}} = V_0' = \sqrt{[V_0^2 - A_0^2]}$. The magnitude of the associated electric field in this frame is $E_{\text{eff}} = E' = V_0'/2W$. From this we can say that the suppression of the creation process can be understood by the Lorentz transformation, as long as the magnetic field has the same spatial dependence as the electric field. We refer to this kind of reduction of pair creation as the *Lorentz suppression*.

One could use the reduced electric field in this moving frame for the Hund approach and compute the transmission coefficient. Equivalently, we have included the magnetic field in the scattering dynamics and determined the transmission. This second approach is more general as it allows us to use arbitrary values, $W_E \neq W_B$, for which the Lorentz transformation based argument is no longer valid. The results for the four rates are summarized in Table II and show that the error of the generalized Hund formula is again less than 3%.

For the third graph [labeled (c)] in Fig. 3 we chose the same electric potential and magnetic field as for graph (b), but the width $W = 0.5/c$ was larger. For this case the effective electric field $E_{\text{eff}} = V_{\text{eff}}/2W = c^2\sqrt{[2.5^2 - 0.6^2]}/(1/c) = 2.43c^3$ is smaller than the effective field $4.13c^3$ of curve (b). Thus, it is not surprising that the corresponding curve (c) is much lower than (b).

To further study the respective roles of the field and potential in the pair-creation process we return to the graph labeled (d), which had identical electric and magnetic fields ($B = 0.6c^3$ and $E = 4.17c^3$) as for graph (b), but a larger width $W = 0.5/c$.
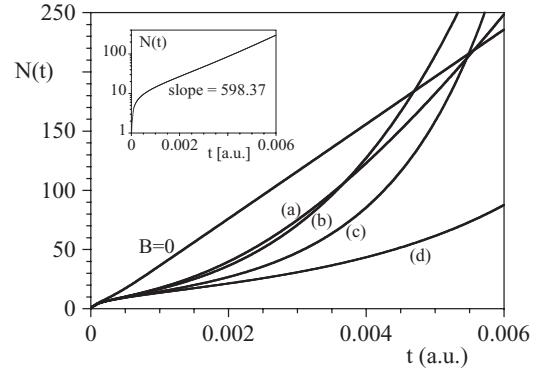

FIG. 4. The number of created bosons as a function of time for four different widths W_B of the magnetic field, while the width $W_E = 0.3/c$ is held constant. We used $W_B c = 1.10$ [for graph (a)], 1.15 (b), 1.25 (c), and 1.30 (d). In the inset we repeat the graph for $W_B = 1.25/c$ with logarithmic scale on the ordinate axis ($V_0 = 2.5c^2$, $B = 0.6c^3$).

Here the number of created particles exceeds even graph (a) for the same electric field but $B = 0$. The effective potential for this configuration, $V_{\text{eff}} = \sqrt{[V_0^2 - A_{y0}^2]} = c^2\sqrt{[4.167^2 - 0.6^2]} \approx 4.124c^2$, is larger than the one for curve (a).

V. EXPONENTIAL INCREASE OF THE BOSONIC PAIR CREATION IN A WIDE MAGNETIC FIELD

While in the previous section the extensions of both fields were identical and smaller than the classical excursion distance, we will now show that the impact of the magnetic field on the bosonic pair creation is qualitatively different if we increase the width W_B beyond W_E. In fact, we will show that the (extraneous) magnetic field *outside* the E-field zone can *increase* the pair-creation process inside this zone.

In Fig. 4 we graph the temporal growth of the bosonic pairs for four different sizes W_B of the magnetic field, all exceeding $W_E = 0.3c^{-1}$. For a comparison, we have also included the graph without any magnetic field.

While for shorter times all graphs reflect the predicted magnetically induced Lorentz suppression as shown in Fig. 3, we observe now that for longer times the number of pairs deviates significantly from the linear growth seen for $W_E = W_B$. In fact, the number of created particles grows exponentially for large times. This is a dramatic difference from the linear results displayed in Fig. 4. We also observe that the growth is nonmonotonic in W_B. In fact, it seems to approach a maximum for about $W_B = 1.25/c$.

In order to show that the increase is indeed exponential, we have graphed in the inset of Fig. 4 the yield $N(t)$ for $W_B = 1.25/c$ with a logarithmic scale on the ordinate axis. The curve is characterized by three time regimes. For early times, the growth of the particle number is associated with the sudden switch on of the electric field at $t = 0$. In the next regime $N(t)$ increases linearly with time. For large times, the growth finally becomes exponential with an exponent γt, where γ is different from R.

The exponential increase of the curves in Fig. 4 is caused by the fact that due to the extra magnetic field outside the interaction zone (of width W_E), the particles can perform a
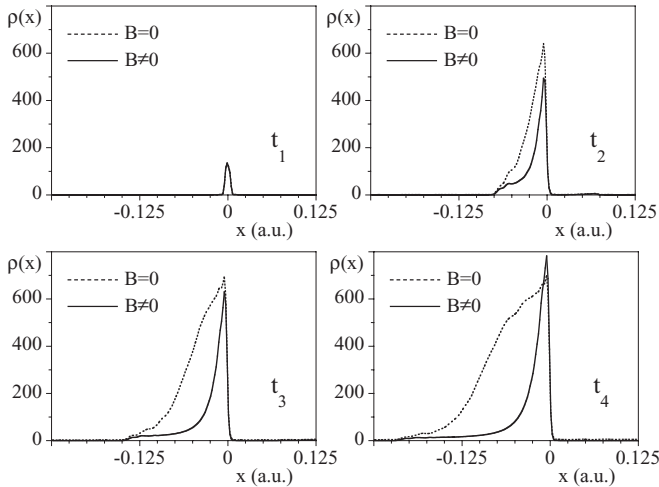
FIG. 5. Comparison of the time evolution of the spatial density with and without the extra magnetic field ($t_1 = 1.5 \times 10^{-5}$ a.u., $t_2 = 5.25 \times 10^{-4}$ a.u., $t_3 = 1.05 \times 10^{-3}$ a.u., $t_4 = 1.575 \times 10^{-3}$ a.u., $V_0 = 2.5c^2$, $W_E = 0.3/c = 0.0022$ a.u., $B = 0.6c^3$, and $W_B = 1.25/c = 0.0091$ a.u.).

cyclotronlike path outside the zone, which permits them to return to the creation zone. Since the returned bosons enhance the creation we find an amplification, which when repeated periodically, leads to an exponential self-amplification of the pair-creation process. Such kind of feedback was not present in the prior cases of Fig. 3 as the magnetic field was too narrow to fully support the cyclotronic orbits and thus not able to bring the bosons back to the creation zone.

The enhancement or lack of enhancement is also manifest in the spatial domain as is shown in the spatial distributions illustrated in Fig. 5. We can see that the presence of the magnetic field causes an obvious suppression at first, but in the long-time limit, the magnetic field restricts the created particles to a cyclotron diameter of about 0.02. We can see that in the interaction zone, namely, the region around $x = 0$, the curve for $B \neq 0$ is higher than the one for $B = 0$. This particle confinement is the reason for the exponential increase in the $N(t)$ graph in Fig. 4. The height of the spatial distributions shows the trend of the exponential enhancement. If the time is sufficiently long, the total number of particles created in combined fields can obviously be much larger than the number of particles created in the electric field only.

VI. SHUT OFF OF THE PAIR PRODUCTION IN THE LARGE WIDTH LIMIT

One could expect that the pair creation should remain to be self-amplifying for any W_B as long as W_B exceeds the excursion distance in the magnetic field. After all, why should an extension of the magnetic field far *outside* the spatial domain of any cyclotron orbit be relevant with respect to the pair-creation process that occurs only *inside* the interaction zone $|x| < W_E$? It turns out that the presence of the magnetic field even in regions that can *never* be visited by a particle is crucially important. In fact, if we continue to increase W_B, we will eventually find a value beyond which the creation of the bosonic particle-antiparticle pairs is completely shut off.
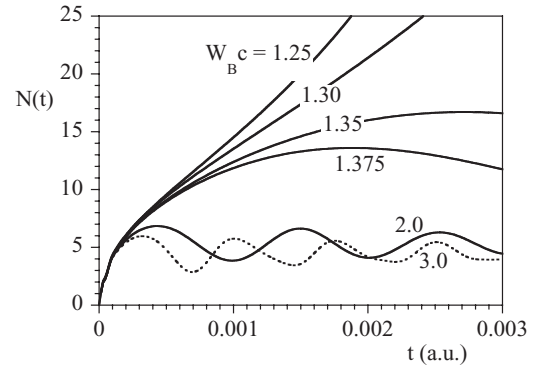

FIG. 6. The total number of created bosons as a function of time for six widths of the magnetic field ($V_0 = 2.5c^2$, $W_E = 0.3/c$, $B = 0.6c^3$, and $L = 1$).

This behavior is shown in Fig. 6. While for $W_B = 1.25/c$ and $1.3/c$ we have the exponential growth already shown in Fig. 4, the graphs for $W_B = 1.35/c$ and $1.375/c$ have a reversed tendency. In fact, the particle numbers for $W_B = 2/c$ and $3/c$ oscillate in time. We therefore have a complete shut off of the pair-creation process if the magnetic field is sufficiently extended. This phenomenon is similar for the fermionic system, which was studied recently [7] and can be best understood in terms of the underlying energy spectra.

A clean analysis of the threshold parameters is difficult to obtain, as the total yield is obtained as the sum over each subdynamics for each canonical momentum p_y. In order to examine the importance of each p_y, we have graphed in Fig. 7 the number of created bosons at a given time t as a function of the canonical momentum.

We can see that only a small number of canonical momenta contribute for the parameters of this simulation. The value of p_y associated with the most particles is close to $-A_0/(2c)$. In fact, particles created within the momentum range $-10.95 - A_0/(2c) < p_y < 10.95 - A_0/(2c)$ account for about 50% of the all particles. We can therefore analyze the behavior of the pair creation for this particular value p_y to predict the behavior of most particles.

In Fig. 8 we have graphed the energy eigenvalues of the Hamiltonian as a function of the spatial size of the
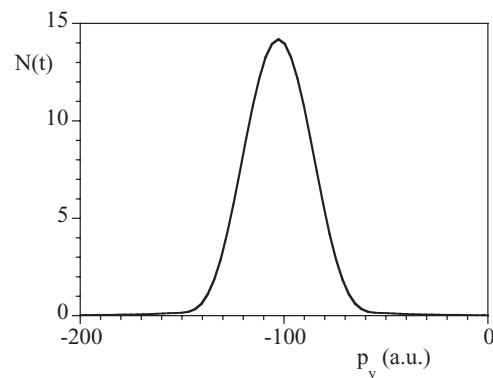

FIG. 7. The number of the created bosons $N(t)$ as a function of p_y at $t = 5.25 \times 10^{-3}$ a.u. for $W_B = 1.25/c$. (The parameters are $V_0 = 2.5c^2$, $W_E = 0.3/c$, and $B = 0.6c^3$.)
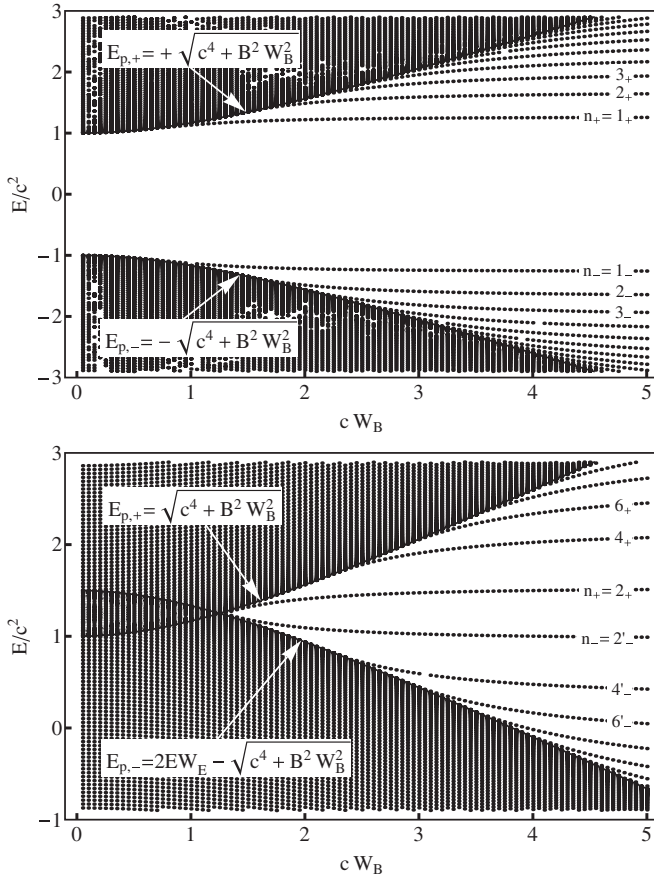
FIG. 8. Energy spectrum of the total Hamiltonian as a function of the spatial size of the magnetic field W_B for the most probable momentum $p_y = -A_0/(2c)$. All parameters are the same as in Fig. 6. The top (bottom) figure shows the spectra for $V_0 = 0$ ($V_0 = 2.5c^2$). It is apparent that when $W_B > 1.25/c$ the two continua begin to separate from each other in the bottom figure. In the band-gap area new discrete energy levels emerge.

magnetic field W_B for the most probable value of the canonical momentum p_y, which is equal to $-BW_B/c$.

To better understand the complicated spectra, the top figure shows the energies in the absence of any electric field. While for $W_B = 0$ the upper and lower edges of the continuum states are given by $E = \pm c^2$, the smallest positive and negative energies are $E = \pm [c^4 + c^2 p_y^2]^{1/2}$ for a nonvanishing width $W_B \neq 0$. As the most likely canonical momentum p_y depends on the vector potential A_0, which, for a constant magnetic field, is a function of the width W_B, then we have $p_y = -BW_B/c$. As a result, the two edges of the continuum energies move apart as the spatial width W_B is increased. We also see the occurrence of several discrete Landau levels.

In the bottom panel we graph the energy levels in the presence of the electric field, associated with $V_0 = 2.5c^2$. For small W_B the positive and negative continuum states overlap as the system is supercritical. As W_B is increased the two edges moved apart, and when W_B is larger than $1.25/c$, the continuum energies begin to separate from each other. The value for W_B when the gap opens again can be calculated by equating the two functions of the continuum edges, $-\sqrt{c^4 + B^2 W_B^2} + 2W_E E = \sqrt{c^4 + B^2 W_B^2}$. If the overlap of

the two energy continua were a necessity for pair creation, we would expect that the creation should stop for $W_B > 1.25/c$. However, our data from Fig. 6 suggest that the pairs are still created for the slightly larger width $W_B = 1.3/c$. The reason for this phenomenon could be that either a different value of p_y is relevant, or that the discrete energy levels are dominant in this regime.

After the opening of the energy gap also several discrete energy levels start to emerge, similar to the Landau states observed on the top panel of the figure. The first discrete level emerges at around $W_B = 0.95/c$. These discrete energy levels are symmetric about the middle. This symmetry is different from the fermion system, as the bosons do not have any spin. The energy spacings between these "electrically dressed" Landau states in the bottom panel are directly related to the temporal oscillations reported in Fig. 6 and we can estimate the frequencies for $N(t)$ in that figure. For example, for $W_B = 3/c$ the energies of the ground state of the negative levels and the ground state of the positive levels would predict an oscillation period of $2\pi/[E(2_+) - E(2_-)] = 7.61 \times 10^{-4}$, which only differs by 2.1% from the observed period of 7.45×10^{-4} in Fig. 6.

VII. DISCUSSION AND OUTLOOK

In summary, we have examined the bosonic particle-antiparticle pair creation for a configuration where the electric and magnetic fields are perpendicular to each other. We allowed both fields to have a spatial dependence in one direction permitting us to study the effect of a localized interaction region on the short- and long-time evolution of the spatial particle density. We observed that depending on the spatial extension of the magnetic field, there are three rather distinct regions that are characterized by either a linear growth, an exponential self-amplification, or a complete shut off of the pair creation. This nonmonotonic behavior is entirely different compared to the corresponding predictions of the Dirac equation for electron-positron pairs.

While the mechanisms leading to the Lorentz suppression of the yield for the case where the electric and magnetic fields have the same spatial extension are understood, the transitions to the beginning and to the end of the exponential self-amplification regime are not. For example, we have argued that the onset of this new regime occurs when the magnetic field outside the interaction region is sufficiently wide to permit the created particles to return to the electric field zone. This argument assumes that we can visualize the quantum field theoretical dynamics in terms of simple classical mechanical orbits. While obviously more quantitative investigations are required, we presently believe that this onset is also accompanied by the occurrence of discrete Landau-bound states in the energy spectrum of the Hamiltonian computed in the absence of the electric field. If the supercritical electric field is included in the spectrum these states become embedded into the upper energy continuum. We plan a more detailed study to examine the precise role these states in the continuum play with respect to the exponential growth. It is also possible that depending on the final energy some states contribute still to the linear growth while others whose spatial distribution is more localized in the interaction region lead to the exponential growth. The

situation gets even more complicated as an entire set of spectra are simultaneously responsible for the whole dynamics, each characterized by the preserved canonical momentum p_y as we have shown above. This complication is also apparent as for the most likely value of p_y the energy continua become separated for $W_B = 1.25/c$, whereas the total number of pairs still grows for slightly larger values of W_B.

Another fascinating question concerns the impact of the created electron-positron pairs on the dynamics during the boson creation. However, a combined theory that could simultaneously take into account the fermionic as well as bosonic particle pairs and their mutual interactions could be attempted only on a very phenomenological level. In any case, in our opinion the perspective of finding a self-amplifying exponential growth is interesting enough to justify further studies.

APPENDIX: QUANTUM BOUNDARY TRANSITION METHOD FOR KLEIN-GORDON SYSTEM

The effective one-dimensional wave function of the boson in the region $x < -L$ and $x > L$, where we choose the scalar potential $V(x)$ and vector potential $A(x)$ as constants, can be written as

$$\psi(x) = \begin{cases} a_0 e^{ip_x x}/\sqrt{2\pi} + a_1 r e^{-ip_x x}/\sqrt{2\pi}, & x < -L \\ a_2 t J e^{-iq_x x}/\sqrt{2\pi}, & x > L, \end{cases} \quad (A1)$$

where the Jacobian $J = E_q p_x)/(E_p q_x)$ and the coefficients a_0, a_1, and a_2 are Klein-Gordon spinors given by

$$a_0 = a_1 = \frac{1}{\sqrt{4E_p c^2}} \begin{pmatrix} c^2 + E_p \\ c^2 - E_p \end{pmatrix}, \quad (A2)$$

$$a_2 = \frac{1}{\sqrt{4E_q c^2}} \begin{pmatrix} c^2 - E_q \\ c^2 + E_q \end{pmatrix}. \quad (A3)$$

Here $E_p = \sqrt{c^4 + c^2(p_x^2 + p_y^2)}$ and $E_q = V_0 - E_p = \sqrt{c^4 + c^2 p_x^2 + c^2(p_y + A_0/c)^2}$, and the Hamiltonian reads

$$h_{\text{KG}} = \begin{pmatrix} \frac{\hat{p}_x^2 + [p_y + A(x)/c]^2}{2} + c^2 + V(x) & \frac{\hat{p}_x^2 + [p_y + A(x)/c]^2}{2} \\ -\frac{\hat{p}_x^2 + [p_y + A(x)/c]^2}{2} & -\frac{\hat{p}_x^2 + [p_y + A(x)/c]^2}{2} - c^2 + V(x) \end{pmatrix}. \quad (A4)$$

If we choose the finite-difference approximation for the operator $\hat{p}_x^2$ as $\hat{p}_x^2 f(x) = -d^2 f(x)/dx^2 = -[f(x_{j+1}) - 2f(x_j) + f(x_{j-1})]/\Delta_x^2$, we have the discretized form of $h_{\text{KG}}\Psi = E\Psi$ as

$$h_{\text{KG}}\psi(x_j) = \begin{pmatrix} \frac{\hat{p}_x^2 + [p_y + A(x_j)/c]^2}{2} + c^2 + V(x_j) & \frac{\hat{p}_x^2 + [p_y + A(x_j)/c]^2}{2} \\ -\frac{\hat{p}_x^2 + [p_y + A(x_j)/c]^2}{2} & -\frac{\hat{p}_x^2 + [p_y + A(x_j)/c]^2}{2} - c^2 + V(x_j) \end{pmatrix} \begin{pmatrix} \psi^1(x_j) \\ \psi^2(x_j) \end{pmatrix}$$

$$= \begin{pmatrix} \frac{-(\psi_{j+1}^1 - 2\psi_j^1 + \psi_{j-1}^1) - (\psi_{j+1}^2 - 2\psi_j^2 + \psi_{j-1}^2)}{2\Delta_x^2} \\ -\frac{-(\psi_{j+1}^1 - 2\psi_j^1 + \psi_{j-1}^1) - (\psi_{j+1}^2 - 2\psi_j^2 + \psi_{j-1}^2)}{2\Delta_x^2} \end{pmatrix}$$

$$+ \begin{pmatrix} \frac{(p_y + A_j/c)^2}{2} + c^2 + V_j & \frac{(p_y + A_j/c)^2}{2} \\ -\frac{(p_y + A_j/c)^2}{2} & -\frac{(p_y + A_j/c)^2}{2} - c^2 + V_j \end{pmatrix} \begin{pmatrix} \psi_j^1 \\ \psi_j^2 \end{pmatrix}$$

$$= E \begin{pmatrix} \psi_j^1 \\ \psi_j^2 \end{pmatrix}, \quad (A5)$$

namely,

$$-(\psi_{j+1}^1 + \psi_{j-1}^1 + \psi_{j+1}^2 + \psi_{j-1}^2) + [\Delta_x^2(p_y + A_j/c)^2 + 2\Delta_x^2 c^2 + 2\Delta_x^2 V_j + 2]\psi_j^1 + [\Delta_x^2(p_y + A_j/c)^2 + 2]\psi_j^2 = 2\Delta_x^2 E \psi_j^1,$$

$$\psi_{j+1}^1 + \psi_{j-1}^1 + \psi_{j+1}^2 + \psi_{j-1}^2 - [2 + \Delta_x^2(p_y + A_j/c)^2]\psi_j^1 - [2 + \Delta_x^2(p_y + A_j/c)^2 + 2\Delta_x^2 c^2 - 2\Delta_x^2 V_j]\psi_j^2 = 2\Delta_x^2 E \psi_j^2. \quad (A6)$$

From Eq. (A6), we have

$$\psi_j^2 = \frac{c^2 - E + V_j}{c^2 + E - V_j} \psi_j^1. \quad (A7)$$

Equation (A7) suggests that only one of the two components is important as the other can be trivially related to the first. From now on, we choose to follow the first component and replace ψ_j^2 using Eq. (A7):

$$-\frac{c^2}{E + c^2 - V_{j-1}}\psi_{j-1}^1 + \frac{\Delta_x^2(cp_y + A_{yj})^2 + 2c^2 + \Delta_x^2(E + c^2 - V_j)(V_j + c^2 - E)}{E + c^2 - V_j}\psi_j^1 - \frac{c^2}{E + c^2 - V_{j+1}}\psi_{j+1}^1 = 0. \quad \text{(A8)}$$

Here we are concerned with the problem of the resonances in an unbounded system. This problem must be formulated in terms of the unbounded scattering states, and to do this we must modify the equation by incorporating the boundary condition. That is, we can add boundary points at $j = 0$ and $j = n + 1$, if we choose the points $j = 1$ and $j = n$ as the limits of the domain in which the potential can vary.

$$\psi_0 = \frac{1}{\sqrt{2\pi}}a_0 e^{i(p_x x_1 - p_x \Delta_x)} + \frac{r}{\sqrt{2\pi}}a_0 e^{-i(p_x x_1 - p_x \Delta_x)},$$

$$\psi_1 = \frac{1}{\sqrt{2\pi}}a_0 e^{ip_x x_1} + \frac{r}{\sqrt{2\pi}}a_0 e^{-ip_x x_1},$$

$$\psi_n = \frac{tJ}{\sqrt{2\pi}}a_2 e^{-iq_x x_n}, \quad \text{(A9)}$$

$$\psi_{n+1} = \frac{tJ}{\sqrt{2\pi}}a_2 e^{-i(q_x x_n + q_x \Delta_x)}.$$

We can get the boundary condition through solving Eq. (A9):

$$\psi_0^1 - e^{ip_x \Delta_x}\psi_1^1 = -\frac{ie^{ip_x x_1}}{\sqrt{2\pi}}\frac{c^2 + E_p}{c\sqrt{E_p}}\sin(p_x \Delta_x),$$

$$\psi_n^1 - e^{iq_x \Delta_x}\psi_{n+1}^1 = 0. \quad \text{(A10)}$$

Considering Eqs. (A8) and (A10), we obtained the extended $n + 2$-dimensional tridiagonal matrix equation that is to be solved:

$$\begin{bmatrix} U_0 & R_1 & & & & & & \\ L_0 & U_1 & R_2 & & & & & \\ & L_1 & U_2 & R_3 & & & & \\ & & \ddots & \ddots & \ddots & & & \\ & & & L_{j-1} & U_j & R_{j+1} & & \\ & & & & \ddots & \ddots & \ddots & \\ & & & & & L_{n-1} & U_n & R_{n+1} \\ & & & & & & L_n & U_{n+1} \end{bmatrix} \begin{bmatrix} \psi_0 \\ \psi_1 \\ \psi_2 \\ \vdots \\ \psi_j \\ \vdots \\ \psi_n \\ \psi_{n+1} \end{bmatrix} = \begin{bmatrix} b_0 \\ b_1 \\ b_2 \\ \vdots \\ b_j \\ \vdots \\ b_n \\ b_{n+1} \end{bmatrix}, \quad \text{(A11)}$$

where we have

$$U_0 = 1,$$
$$R_1 = -e^{ip_x \Delta_x}, \quad \text{(A12)}$$

$$L_{j-1} = -c^2/(E + c^2 - V_{j-1}) \quad (j = 1,2,3,...,n),$$

$$U_j = \frac{\Delta_x^2(cp_y + A_{yj})^2 + 2c^2}{E + c^2 - V_j} + \Delta_x^2(V_j + c^2 - E) \quad (j = 1,2,3,...,n), \quad \text{(A13)}$$

$$R_{j+1} = -c^2/(E + c^2 - V_{j+1}) \quad (j = 1,2,3,...,n),$$

$$L_n = 1,$$
$$U_{n+1} = -e^{iq_x \Delta_x}, \quad \text{(A14)}$$

$$b_0 = -\frac{ie^{ip_x x_1}}{\sqrt{2\pi}}\frac{c^2 + E_p}{c\sqrt{E_p}}\sin(p_x \Delta_x),$$

$$b_k = 0 \quad (k = 1,2,3,\ldots,n+1). \quad \text{(A15)}$$

When the matrix equation (A11) is inverted, we obtain the value of Ψ_n and then the transmission coefficient can be computed according to

$$T(E) = 8\pi c^2 E_q |\Psi_n|^2 / J / (c^2 - E_q)^2. \tag{A16}$$

[1] F. Sauter, Z. Phys. **69**, 742 (1931); **73**, 547 (1931).
[2] J. Schwinger, Phys. Rev. **82**, 664 (1951).
[3] For a recent review, see A. Di Piazza, C. Müller, K. Z. Hatsagortsyan, and C. H. Keitel, Rev. Mod. Phys. **84**, 1177 (2012).
[4] For early work on bosonic and fermionic pair creation rates, see E. Brezin and C. Itzykson, Phys. Rev. D **2**, 1191 (1970); N. B. Narozhny and A. I. Nikishov, Sov. Phys. JETP **38**, 427 (1974).
[5] For experimental proposals, see, e.g., http://www.extreme-light-infrastructure.eu/.
[6] W. Greiner, B. Müller, and J. Rafelski, *Quantum Electrodynamics of Strong Fields* (Springer Verlag, Berlin, 1985).
[7] Q. Su, W. Su, Q. Z. Lv, M. Jiang, X. Lu, Z. M. Sheng and R. Grobe, Phys. Rev. Lett. **109**, 253202 (2012).
[8] Q. Lin, J. Phys. G **25**, 17 (1999).
[9] G. Dunne, in *From Fields to Strings*, edited by M. Shifman, Vol. 1 (World Scientific, 2004), p. 445.
[10] N. Tanji, Ann. Phys. (Leipzig) **324**, 1691 (2009).
[11] A. Hansen and F. Randal, Phys. Scr. **23**, 1036 (1981).
[12] C. A. Manogue, Ann. Phys. **181**, 261 (1988).
[13] B. R. Holstein, Am. J. Phys. **66**, 507 (1998).
[14] N. Dombey and A. Calogeracos, Phys. Rep. **315**, 41 (1999).
[15] P. Krekora, Q. Su, and R. Grobe, Phys. Rev. Lett. **92**, 040406 (2004).
[16] P. Krekora, K. Cooley, Q. Su, and R. Grobe, Phys. Rev. Lett. **95**, 070403 (2005).
[17] R. E. Wagner, M. R. Ware, Q. Su, and R. Grobe, Phys. Rev. A **81**, 024101 (2010).
[18] R. E. Wagner, M. R. Ware, Q. Su, and R. Grobe, Phys. Rev. A **81**, 052104 (2010).
[19] F. Hund, Z. Phys. **117**, 1 (1941).
[20] W. Su, M. Jiang, Z. Q. Lv, Y. J. Li, Z. M. Sheng, R. Grobe, and Q. Su, Phys. Rev. A **86**, 013422 (2012).
[21] H. Feshbach and F. Villars, Rev. Mod. Phys. **30**, 24 (1958).
[22] For a review on the properties of the Klein-Gordon Hamiltonian, see, e.g., W. Greiner, *Relativistic Quantum Mechanics*, 3rd ed. (Springer, Berlin, 2000); A. Wachter, *Relativistische Quantenmechanik* (Springer, Berlin, 2005).
[23] J. W. Braun, Q. Su, and R. Grobe, Phys. Rev. A **59**, 604 (1999).
[24] G. R. Mocken and C. H. Keitel, Comput. Phys. Commun. **178**, 868 (2008).
[25] M. Ruf, H. Bauke, and C. H. Keitel, J. Comput. Phys. **228**, 9092 (2009).
[26] For a review of the one-dimensional Dirac equation, see, e.g., T. Cheng, Q. Su, and R. Grobe, Contemp. Phys. **51**, 315 (2010).
[27] M. Leng and C. S. Lent, J. Appl. Phys. **76**, 2240 (1994).